Electrochemically stable carbazole-derived polyaniline for pseudocapacitors

Mohammed Almtiri, Timothy J. Dowell, Hari Giri, David O. Wipf, and Colleen N. Scott*

Department of Chemistry, Mississippi State University, Starkville, Mississippi 39762, USA cscott@chemsitry.msstate.edu

ABSTRACT: Supercapacitor energy storage devices are well suited to meet the rigorous demands of future portable consumer electronics (PCEs) due to their high energy and power densities (i.e., longer battery-life and rapid charging, respectively) and superior operational lifetimes (ten times greater than lithium-ion batteries). To date, research efforts have been narrowly focused on improving the specific capacitance of these materials; however, emerging technologies are increasingly demanding competitive performance with regards to other criteria, including scalability of fabrication and electrochemical stability. In this regard, we developed a polyaniline (PANI) derivative that contains a carbazole unit co-polymerized with 2,5-dimethyl-p-phenylenediamine (**Cbz-PANI-1**) and determined its optoelectronic properties, electrical conductivity, processability, and electrochemical stability. Importantly, the polymer exhibits good solubility in various solvents, which enables the use of scalable spray-coating and drop-casting methods to fabricate electrodes. **Cbz-PANI-1** was used to fabricate electrodes for supercapacitor devices and exhibits a maximum areal capacitance of 64.8 mF cm⁻² and specific capacitance of 319 F g⁻¹ at a current density of 0.2 mA cm⁻². Moreover, the electrode demonstrates excellent cyclic stability (\approx 83% of capacitance retention) over 1000 CV cycles. Additionally, we demonstrate the charge storage performance of **Cbz-PANI-1** in a symmetrical supercapacitor device, which also exhibit excellent cyclic stability (\approx 91% of capacitance retention) over 1000 charge-discharge cycles.

KEYWORDS: polyaniline, carbazole, conducting polymer, redox polymer, supercapacitor.

INTRODUCTION

Polyaniline (PANI) is one of the most studied conducting polymers (CPs) to date. Its many attributes include easy and inexpensive preparation, non-redox doping, environmental stability in the doped state, reversible oxidative states, and high electrical conductivity. As a result, PANI is being explored for application in many fields such as sensors, 1-2 devices,3-5 corrosion storage inhibitor,6-8 photovoltaic cells,9-11 and microwave safeguards and electromagnetic shielding materials.12-13 However, PANI is challenged with two main problems; it undergoes electrochemical aging, which results in electrochemical instability and it is insoluble in common organic solvents. 14-¹⁶ Reported approaches that render PANI soluble include incorporating solubilizing counterions and blending with solubilizing polymers. 17-18 Recently, Mustafin et al. reported PANI derivatives with short alkyl chains that were soluble in common organic solvents. While there have been several approaches to address PANI's insolubility, there are fewer reports that address its electrochemical instability. The common approach is to dope the polymer with large counter ions or prepare nano-structures. 19-20 However, these approaches have not been overwhelming successful. Recently, we reported a PANI-derivative containing a phenoxazine moiety that was stable over 100 CV cycles without noticeable degradation.²¹ However, phenoxazine is expensive and requires a multi-step synthesis for its

preparation. Consequently, carbazole was investigated as a replacement for phenoxazine as a PANI derivative (Cbz-PANI) due to its low cost, facile side-chain modification at the nitrogen 9H-position to increase solubility, and ease of functionalization at the 3- and 6- positions for further reactivity.²²⁻²³ As such, Cbz-PANI derivatives can be prepared on large scale. Carbazoles are also used as charge transport materials because they easily form relatively stable cations with high charge carrier mobility.²⁴ Homopolymers prepared from carbazole such as 3,6polycarbazole²⁵⁻²⁶ and 2,7-polycarbazole²⁷ were explored for their electrochromic and photoreactive properties. Additionally, the carbazole core was combined with other monomers such as 3,4-ethylenedioxythiophene (EDOT),28 thiophene (Th),²⁹ phenylene (Ph),³⁰ and diphenylvinylene (DPV),31 which are known for their diverse optical,22 electrochemical,^{23, 32-33} and conducting properties.²⁸ Yet, to the best of our knowledge, there is only one report of a π conjugated carbazole homopolymer, produced by the homopolymerization of 9-methyl-9*H*-carbazol-3-amine monomer that was explored as a fluorescent chemosensor; however, its electrochemical properties were not described.34

Over the last decade, there has been a push to expand electrified transportation and renewable energy production (e.g., wind and solar), which has increased the demand for batteries (high energy density) and

storage devices.35 However, there is a need for both highenergy and high-power density in a single device and supercapacitors (SC) can achieve both. Many materials such as metal oxides, metal-organic frameworks, MXenes, carbon-based nanomaterials, and CPs have been evaluated as SC materials;³⁶⁻³⁸ however, the high cost, low capacitance, and instability of the devices are common problems with such materials.^{37, 39} Among the list of SC materials, CPs are attractive for flexible energy storage devices, due to their synthetic structural diversity, wide range of tunable properties (e.g., electrical, mechanical, electrochemical, and optical) and their potential for scalable device fabrication.⁴⁰ The redox activity (i.e., pseudocapacitive energy storage) of CPs can be controlled by tailoring the chemical structure of the polymer backbone. In this regard, numerous CPs; for example, PANI, polypyrrole (PPy), polythiophene (PTh), and their derivatives have been prepared and studied as SC materials.41-43 Among these, PANI is one of the most rigorously studied and promising CPs for SC applications due to its redox properties, wide operational window in aqueous electrolyte (≥ 1 V), facile preparation, high conductivity, and relatively low cost.44 In fact, polyaniline electrodes have recorded one of the highest values for polymer-based electrodes with a specific capacitance >1000 F g⁻¹, which is comparable to costly rare metals (ruthenium oxide (1170 F g⁻¹)) and significantly better than commercial activated carbon (AC) electrodes (<200 F g⁻¹).⁴⁵ However, these high performing PANI SC typically consist of conductive additives and binders, or they have been structurally ordered into nano materials to attain high surface areas.46-48 For example, a pseudocapacitor fabricated from a three-dimensional network structure of cellulose nanofibers (CNFs), carbon nanotubes (CNTs), PANI, and carbon cloth (CC) produced a specific capacitance of 318 F g^{-1} at a scan rate of 10 mV s^{-1} with a 72% retention in performance after 1000 cycles.⁴⁹ Alternatively, PANI based pseudocapacitors prepared without conductive additives or special structural arrangements, usually result in lower specific capacitance. For example, a pseudocapacitor based on electrochemically deposited PANI on stainless steel mesh recorded capacitance of 282 F g⁻¹ within a wide voltage window of 0–1.4 V.⁵ Additionally, a stretchable SC made from PANI/graphene electrodes displayed a maximum specific capacitance of 261 F g-1 and a 89% capacitance retention over 1000 charge-discharge cycles at 1 mA cm-2.50 PANI, like most CPs, undergoes swelling/shrinking during charge/discharge cycling, which can result in a slow electrochemical degradation and significant impaired capacitances after charge/discharge cycles.51 Thus, the practical application of PANI (and other CPs) as SC material has been impeded by its electrochemical instability.16 Furthermore, the low solubility of PANI in common solvents severely limits the

electrochemical capacitors (high power density) charge

type of fabrication technique available to prepare devices; typically, electropolymerization is the preferred method for depositing PANI polymers as films on electrodes. While obtaining a high specific capacitance for SC materials is the primary focus of many reports, factors such as long-term cycling stability, mechanical robustness, and scalability of fabrication are needed for commercial viability.⁴⁰

In this manuscript, we describe our strategy to prepare economical, electrochemically stable, and processable PANI-derivatives from carbazole and 1,4aryldiamines (Cbz-PANI) SC for device. Buchwald/Hartwig coupling reaction was used to prepare the polymers, poly(9-(2-ethylhexyl)-carbazole-3,6-diyl-alt-2,5-dimethyl-p-phenylenediamine) (**Cbz-PANI-1**), and poly(9-(2-hexyldecyl)-carbazole-3,6-diyl-alt-p-phenylenediamine) (Cbz-PANI-2). These polymers are soluble in many common organic solvents, which permit their full characterization and allow for solution processing. The chemical structures of the polymers were confirmed by ¹H NMR and FTIR. Furthermore, the Cbz-PANI-1 demonstrated favorable redox activity and high electrochemical stability when examined by 3-electrode cyclic voltammetry (CV), galvanostatic charge-discharge (GCD), and as a symmetric two-electrode SC device. The high solubility of Cbz-PANI-1 enables it to be spray-coated or drop-casted onto indium tin oxide (ITO) coated glass substrates and homemade flexible gold-leaf coated PET substrate (Au@PET, 24k Au leaf on single sided PET laminate), providing a potential high-throughput processing route for large scale flexible device fabrication.

EXPERIMENTAL

General: All reagents were purchased from commercial sources and used without further purification unless otherwise stated. All chemicals were standard reagent grade unless otherwise specified. The solvents used in the synthesis (THF, DMF, and toluene) were distilled over drying agents. The reactions were carried out in oven-dried glassware. Air or moisture susceptible reactions were performed under inert atmosphere (nitrogen or argon gas) in the glovebox.

Nuclear Magnetic Resonance (NMR) spectra were recorded at 500 MHz for the ¹H NMR spectrometer and 126 MHz for the ¹³C NMR on a Bruker spectrometer at room temperature in deuterated solvents. The NMR data were processed by MestReNova and the chemical shifts were expressed in parts per million (ppm) downfield from SiMe₄ (0.0 ppm). CDCl₃ reference peak was taken at 7.26 ppm for ¹H NMR or 77.0 ppm for ¹³C NMR. CDCl₃ was used as the solvent for all compounds unless there was an overlap with the compound peak, upon which another solvent was used as noted in the NMR data. The coupling constants (J) were expressed in Hz. Multiplicities were expressed as: s (singlet); d (doublet); t

(triplet); q (quartet), m (multiplets). The products were purified by flash chromatography on CombiFlash Rf+ Purlon with silica gel (300-400 mesh) having 60 Å pore size. Commercially packed flash columns were obtained from Silicycle. Thin-layer chromatography (TLC) was done on 50 mm × 20 mm aluminum-backed silica gel and visualized with a UV lamp at 254 nm. Thermogravimetric analyses (TGA) were performed on a TA Q50. Infrared spectra (ATR-FTIR) of powder polymers were obtained on a Cary 630 provided with a Diamond Attenuated Total Reflectance (ATR) accessory and data are expressed in wavenumbers (cm⁻¹). Scanning electron microscope (SEM) images were performed with Jeol JSM-6500F field emission with 15 kV accelerating voltages. The SEM samples were prepared by substrate. Electrochemical on Au leaf characterization was carried out at ambient temperature in a standard three-electrode cell and two electrode assembles with a Versastat-3 potentiostat/galvanostat. Platinum disc, glassy carbon, ITO (7 mm × 50 mm × 0.7 mm), or 24k Au leaf on single sided PET laminate (Au@PET) were taken as the working electrodes and platinum wire (having dimension 25 × 35 mm) as the counter electrode. The working electrodes were spray-coated or drop-casted with the polymer to form thin films. The reference electrode was Accumet glass body Ag/AgCl electrode. The electrical conductivity of polymer film was measured with a fourpoint collinear probe with 0.2-inch probe distance. Custom software collected the conductivity data using a Keithley 6221 current source and a Keithley 6512 electrometer.

Carbazole monomer synthesis:

General procedure for compounds 1a - b.52-53

Carbazole (1.00 g, 5.98 mmol) was charged in an oven-dried two-necked round-bottom flask along with NaH (0.2 g, 8.37 mmol) in DMF (25 mL) as solvent. The mixture was stirred for 30 min under nitrogen flow. Alkyl bromide (1.2 eq) was added dropwise for 30 min, and the reaction mixture was heated in an oil-bath at 100 °C overnight. The reaction was allowed to come to rt before quenching with aliquots of water and extracted three times with dichloromethane. The combined organic layer was further washed with brine, and the residual water was absorbed by anhydrous Na₂SO₄ and filtered. The filtrate was concentrated under reduced pressure and purified by silica gel flash chromatography with hexane as the mobile phase.

General procedure for compounds 2a - b.52-53

The product (1a) (2 g, 7.16 mmol) was added to CHCl $_3$ (50 mL) in a 250 mL two-necked round-bottom bottom flask and the reaction mixture was covered (i.e., wrapped in aluminum foil). Then N-bromosuccinimide (NBS) (2.8 g, 15.7 mmol) was gradually added to the reaction in an ice-

bath at 0 °C. The reaction mixture was stirred overnight at rt. The mixture was quenched by adding aliquots of water. The product was extracted with DCM (3 × 100 mL), washed with brine and dried over anhydrous MgSO $_4$. The solvent was removed under reduced pressure and the product was purified by flash chromatography on silica gel using hexane as the mobile phase.

General procedure for Cbz-PANI-1 and Cbz-PANI-2:

An oven-dried microwave tube containing a magnetic stir bar was charged in the glove box with 3,6-dibromo-9-(2ethylhexyl)-carbazole (2a) (0.350 g, 1.0 eq.), 2,5-dimethylp-phenylenediamine (0.110 g, 1.05 eq.), Pd(OAc)₂ (0.089 g, 0.05 eq.), Brettphos (0.032 g, 0.075 eq.), and NaO'Bu (0.215 g, 2.8 eq.). The microwave tube was capped and remove from the glovebox. Freshly distilled dried THF (5 mL) was added, and the reaction was stirred vigorously while heating at 85 °C in an oil bath for 24 h. The reaction was allowed to cool to rt and diluted with DCM. The crude polymer was filtered through Celite, and the filtrate was evaporated under reduced pressure to give the solid crude polymer. The polymer was further purified by soxhlet extraction with methanol, acetone, hexanes, and extracted with dichloromethane. The polymers were obtained in 93% and 81% for Cbz-PANI-1 and Cbz-PANI-2, respectively.

Electrochemical Characterization

Electrodes were fabricated by preparing an 85:15 wt/wt Cbz-PANI-1/PSS (polymer/dopant) ethanol solution at a concentration of 5 mg/mL, which was spray-coated onto homemade gold-leaf coated PET (Au@PET, 24k Au leaf on single sided PET laminate). Cbz-PANI-1 was spray-coated onto a 2 cm × 4 cm Au@PET substrate, and then cut into eight individual 1 x 1 cm area Cbz-PANI-1/Au@PET electrodes. The average active material mass loading was determined to be ≈0.3 mg cm⁻², which was used to calculate areal and gravimetric performances of the material/device. The relatively small mass of material deposited (≈ 2.4 mg/8 cm²) compared to the analytical balance resolution (0.1 mg) prompted an analysis of the expected error in the mass loading. Using standard methods for error propagation, the relative error in mass loading was calculated to be 11%. The spray coated Cbz-PANI-1/Au@PET was employed as the working electrode during three-electrode configuration measurements in aqueous 1 M H₂SO₄ solution where carbon fiber cloth was used as the counter electrode and Ag/AgCl as the reference electrode. However, for the cyclability measurements the Au leaf was immersed in 2-methyl-1propanethiol for ten minutes before dropped casting the polymer. The treatment of the gold-leaf with thiol notably enhanced the interfacial adhesion strength between Au leaf and the polymer material and the drop-casting method

increased the amount of polymer on the gold-leaf (\approx 300 mg).

Device Fabrication and Electrochemical Evaluation

Cbz-PANI-1/Au@PET electrodes (3 cm \times 1 cm) were prepared by spray-coating the polymer onto a masked 1 cm² area of the Au@PET substrate. The electrodes were assembled into a symmetric supercapacitor device using double-side tape (acting as spacer and adhesive) so that only the polymer coated area (1 cm²) remained exposed. Prior to assembly, a small drop of H_2SO_4/PVA polymer gel electrolyte was placed on the exposed area of each electrode. For the cyclability measurements, a set of ten similarly fabricated devices were prepared and tested by extended galvanostatic charge discharge for 1000 cycles and the best cell performance was further analyzed.

RESULTS AND DISCUSSIONS

We recently reported the synthesis of a phenoxazine PANI derivative that showed excellent electrochemical stability.21 However, phenoxazine is expensive and its preparation requires a multi-step approach. Herein, we investigate carbazole as an inexpensive replacement for phenoxazine in preparing electrochemically stable and processable PANI derivatives. In our previous study, we demonstrated the utility of the Buchwald/Hartwig coupling reaction to synthesize our polymers. Herein, we expand on the use of the this approach to prepare two more PANI derivatives from carbazole and 1,4-aryldiamines comonomers. The polymers, poly(9-(2-ethylhexyl)-carbazole-3,6-diyl-alt-2,5-dimethyl-p-phenylenediamine) (Cbz-PANI-1), and poly(9-(2-hexyldecyl)-carbazole-3,6-diyl-alt-pphenylene-diamine) (Cbz-PANI-2), were prepared from the carbazole monomers 2a and 2b, respectively (Scheme 1). The carbazole monomers were synthesized in two steps from carbazole, which were then subjected to the Buchwald/Hartwig cross-coupling reaction with 2,5dimethyl-p-phenylenediamine (DMPPDA) to give Cbz-**PANI-1** and *p*-phenylenediamine (PPDA) to give **Cbz-PANI-**2 according to Scheme 1. The polymerization conditions were optimized with Cbz-PANI-1 to obtain a highest molecular weight while limiting the formation of the undesirable insoluble fractions, which is believed to come from the over-arylation of the secondary amine to form undesired cross-linked tertiary amines (Scheme-S1).54 To optimize the polymerization conditions, we decided to examine both monodentate dialkylbiaryl phosphine and bidentate ligands, which have been reported as highly efficient ligands in the Pd-catalyzed C-N bond formation.55 shown Table-S1. Run 1 tris(dibenzylideneacetone)dipalladium(0) (Pd(dba)₂) complex catalyst and either 2,2'-bis(diphenylphosphino)-1,1'-binaphthyl (BINAP) 1,1'-ferrocenediylor

bis(diphenylphosphine) (DPPF) as the ligands, only produced oligomers or low molecular weight polymers (M_n ≈3 – 4 kDa) with no sign of the over-arylation product. Significantly better results were obtained using the monodentate dialkylbiaryl phosphine ligand, dicyclohexylphosphino-2',4',6'-triiso-propylbiphenyl (Xphos), with palladium acetate (Pd(OAc)₂) as the catalyst. Under these conditions, the M_n increased dramatically reaching ≈13 kDa; however, insoluble polymers were also obtained (Table S1, Run 3). Improvement in the M_n (18 kDa) of the polymer occurred by employing 2-(dicyclohexylphosphino)3,6-dimethoxy-2',4',6'- triisopropyl-1,1'-biphenyl (Brettphos) as the ligand and Pd(OAc)₂ as the catalyst (Table S1, Run 4).56 Consequently, both polymerization reactions were carried out in dry THF with Pd(OAc)₂/Brettphos as the catalyst/ligand system and NaOtBut as the base at 85°C for 24 h (Scheme 1). Upon opening the reaction vials to expose the content to air, a gradual color change occurred from brown to purple. From our previous experience with the phenoxazine PANIderivative, we believe this color change indicates partial oxidation of the polymer from the analogous leucoemeraldine base of PANI to the analogous emeraldine base form. To test our hypothesis, an absorption spectrum of the brown colored polymer was obtained by a quick workup of the reaction under nitrogen atmosphere. The absorption spectrum is consistent with the analogous leucoemeraldine base of PANI (**Figure-S1**).⁵⁷ The polymers were purified by soxhlet extraction with methanol, acetone, hexane, and collected in dichloromethane. The fractionated polymers were analyzed by gel permeation chromatography (GPC) at 40 °C in THF with polystyrene standards. A moderate molecular weight (MW) (Mn ≈18 kDa, PDI 1.48) was obtained for Cbz-PANI-1, but a low MW $(M_n \approx 9 \text{ kDa}, \text{PDI } 1.37)$ was obtained for **Cbz-PANI-2**. The low M_n for Cbz-PANI-2 is a result of the polymer's insolubility in the reaction solvent even when the large 2hexyldecyl side chain was used.

Scheme 1 Synthesis of Cbz-PANI-1 and Cbz-PANI-2

¹H NMR spectra for **Cbz-PANI-1** and **Cbz-PANI-2** are illustrated in Figure 1. The peaks pertaining to the alkyl groups (CH₃ and CH₂) can be found between 0.75 and 1.5 ppm for Cbz-PANI-1 and 0.5 to 1.5 ppm for Cbz-PANI-2. The methyl protons on the PPDA in Cbz-PANI-1 can be found around 2.25 ppm and the methine (CH) and methylene (CH₂) protons of the branched alkyl chains resonate around 2.10 and 2.0 ppm and 4.25 and 4.0 ppm for Cbz-PANI-1 and Cbz-PANI-2, respectively. The aromatic regions for both polymers give broad indistinguishable peaks. The FTIR spectra for both polymers are shown in Figure S2. The FTIR spectra are consistent with previous PANI structures.⁵⁸⁻⁵⁹ The absorption bands at around 3150 cm⁻¹ represent the stretching vibrations of the N-H bonds for the polymers' emeraldine bases and salts. The C-H stretching of aromatic rings at 3044 cm⁻¹ and the C-H stretching of alkyl chains between 2940 and 2830 cm⁻¹ are also present in the high-frequency area. The C-C stretches of the quinoid and benzenoid rings are assigned to the peaks at 1553 and 1472 cm⁻¹ in Cbz-PANI-1. The C-N stretching vibration of the quinoid-benzenoid-quinoid (QBQ) vibration is attributed to the peak at 1368 cm⁻¹, while the para-substituted benzene rings have out plane deformation C-H deformation at 804 cm⁻¹. Cbz-PANI-2 follows a similar pattern.

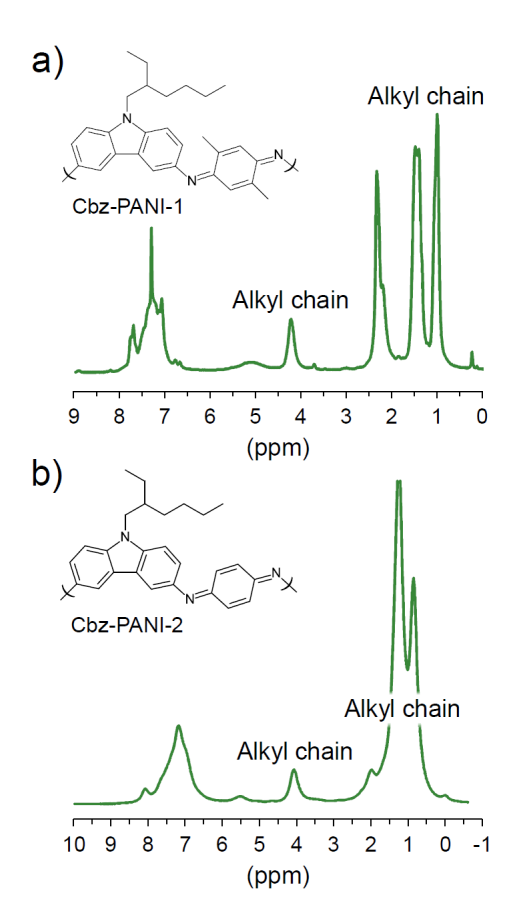


Figure 1. ¹H NMR spectra for **Cbz-PANI-1** (a) and **Cbz-PANI-2** (b).

The UV/vis-NIR absorption spectra of the doped and undoped forms of the polymers were recorded in organic solvents. The polymers were isolated in their partially oxidized basic forms, which is analogous to PANI emeraldine base (EB). This basic form of the polymer, when doped with acid, forms the analogous PANI emeraldine salt (ES). **Figure 2** shows the absorption spectra for CSA-doped Cbz-PANI-1 and Cbz-PANI-2 as a representative of the other doped polymers. A characteristic π - π * absorption band for the EB form can be seen at 317, and 319 nm for Cbz-PANI-1 and Cbz-PANI-2, respectively, while the same transitions for the ES forms were located at 390 and 395 nm, respectively (Figure 2a). A second transition is observed in the visible region for EB form at 573 for Cbz-PANI-1 and 580 for Cbz-PANI-2 that are attributed to the charge transfer from benzoid to the quinoid structure. This transition is not observed in the doped polymer; however, a new transition in the near infrared region (NIR) around 890 and 911 nm was observed for Cbz-PANI-1 and Cbz-PANI-2, respectively. These peaks are attributed to the polaron

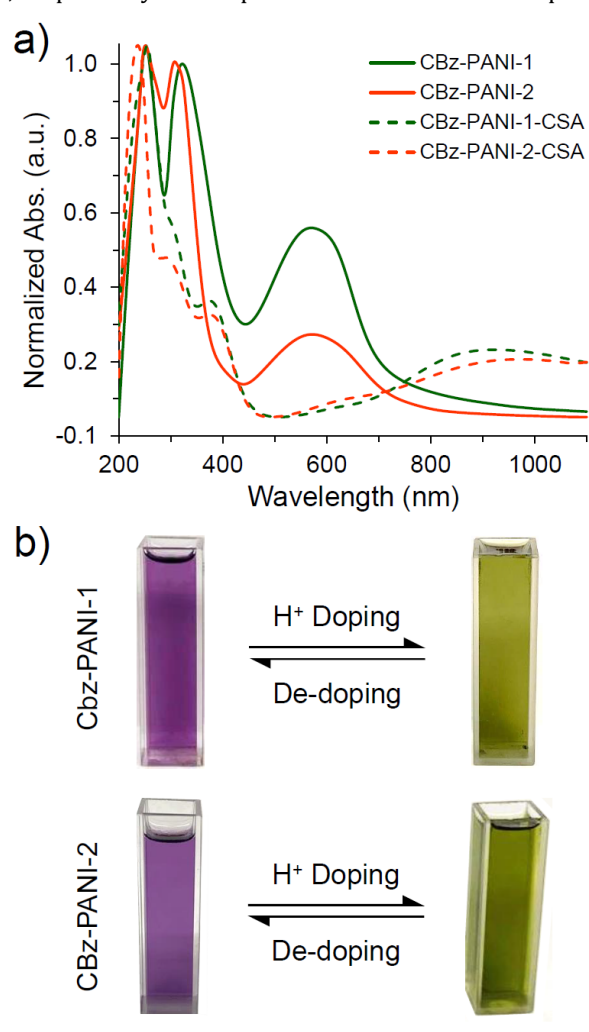


Figure 2. Absorption spectra for the undoped (CHCl₃) and doped (EtOH) states of **Cbz-PANI-1** and **Cbz-PANI-2**, (a); Colors of the undoped and doped **Cbz-PANI-1** and **Cbz-PANI-2** (b).

band transitions. 60-61 **Figure 2b** shows the color change for the EB and ES forms of the polymers, which goes from pink/purple to green. The effects of different dopants on the polymers are shown in Figure S3. From the absorption spectra, the acids were all effective dopants for the polymers; however, camphorsulfonic acid (CSA) and polystyrene sulfonate (PSS) were chosen as the dopants for future studies because they were more thermally stable during the annealing process than films doped with trifluoroacetic acid (TFA), dodecylbenzene sulfonic acid (DBSA), and hydrochloric acid (HCl). During the annealing process, the TFA and DBSA doped polymers were de-doped as seen by the change in the films' color; on the other hand, the HCl doped polymer does not make effective films. Based on the thermogravimetric analysis data (Figure S4), where the decomposition of the polymer occurs over 400 °C, it is

clear that the polymers are stable at the annealing temperature of $80 - 100 \, ^{\circ}\text{C}$.

EPR measurements were performed to detect the existence of paramagnetic species due to unpaired electrons in the doped state as would be expected if polarons are present. Both polymers recorded strong signal in the EPR spectra when doped with organic acids (**Figure S5a** and **c**) and showed Curie behavior with temperature (**Figure S5b** and **d**). The g-factors ranged from 2.0010 to 2.0063 G, which are close to the value for free electrons, suggesting that the resonances of the paramagnetic centers are delocalized over the conjugated polymers.⁶²⁻⁶³ From the EPR studies, the presence of paramagnetic charged states (polarons) was confirmed for the doped polymers. As such, the electrical conductivity of the polymers was determined

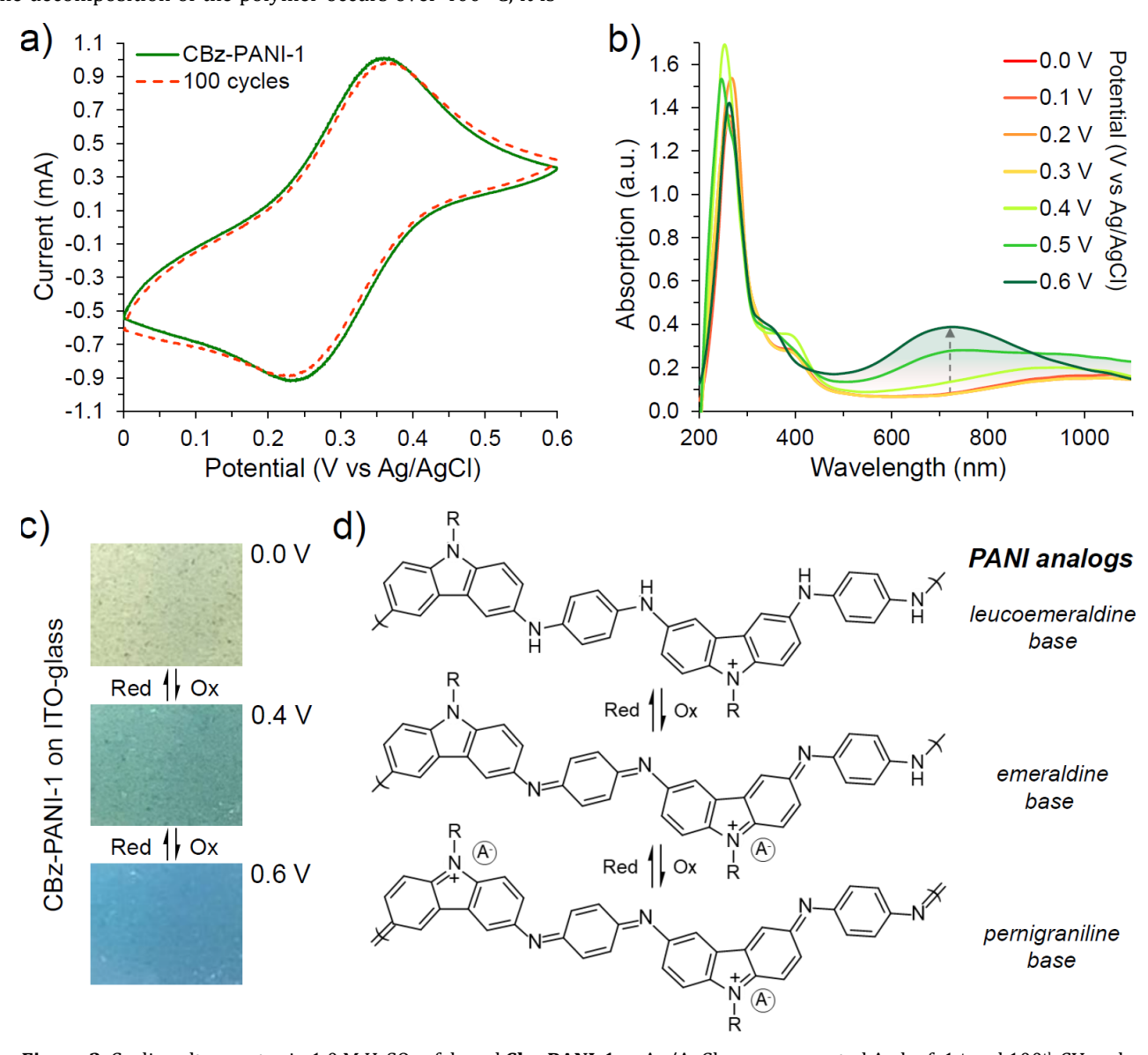


Figure 3. Cyclic voltammetry in 1.0 M H₂SO₄ of doped **Cbz-PANI-1** vs Ag/AgCl on spray-coated Au leaf; 1^{st} and 100^{th} CV cycles shown (a). Spectroelectrochemical measurements of **Cbz-PANI-1** from 0.0 to 0.6 V of spray-coated polymer films on conductive ITO coated glass (b). Electrochromic changes for **Cbz-PANI-1** between the leucoemeraldine salt (0.0 V), emeraldine salt (0.4 V), and the pernigraniline salt (0.6 V) (c). Proposed redox forms for **Cbz-PANI** (d).

using a four-point probe apparatus. Films of **Cbz-PANI-1** and **Cbz-PANI-2** were prepared by drop-casting a 5 mg/mL EtOH solution of the polymers onto the substrate, which were then subjected to slow drying over *m*-cresol vapor at 100 °C for 24 h. In our previous studies, it was shown that *m*-cresol increased the conductivity by changing the morphology of the polymers from aggregated particles to thick sheet-like structures.²¹ The conductivity was determined to be 2.82 S cm⁻¹ for **Cbz-PANI-1** and 0.70 S cm⁻¹ for **Cbz-PANI-2**. The reason for the lower conductivity of **Cbz-PANI-2** is a result of the lower M_n of the polymer, which results in a less efficient film.⁶⁴ Based on the conductivity studies, we decide to perform electrochemical experiments using **Cbz-PANI-1**.

Cyclic voltammetry (CV) of a **Cbz-PANI-1** film between 0 and 0.6 V (vs Ag/AgCl) shows redox peaks centered between 0.37 V (Ep_a) and 0.25 V (Ep_c) at the scan rate of 200 mV s⁻¹ (**Figure 3a**). The electrochemical stability of the polymer can be seen from the 100^{th} cycle (red dashed line) in which the overall change in shape and current density are minimal compared to the 1^{st} cycle (**Figure 3a**).

Spray-coated polymer films on conductive ITO coated glass (ITO@glass) were analyzed using spectroelectrochemistry (Figure 3b). As expected, the polymer showed electrochromic properties between 0.00 and 0.60 V vs Ag/AgCl. The films appear faintly yellow/green in their reduced state (0.0 V), transition to green when partially oxidized (0.4 V) and become blue when fully oxidized (0.6 V) (Figure 3c). In the process, the maximum absorption wavelength shifts from 1000 nm in the ES form to 720 nm in the oxidized pernigraniline state. This blue shift in the wavelength of the fully oxidized polymer is a result of Peierls gap, which has been previously described in the literature for the pernigraniline form of PANI.⁶⁵⁻⁶⁶ The proposed structures for the different redox states can be seen in Figure 3d.

Cyclic voltammetry experiments were also carried out between 0 and 0.6 V (vs Ag/AgCl) at various scan rates (10 to 200 mV s $^{-1}$) for **Cbz-PANI-1** as shown in **Figure 4a**. The positive potential window (from 0.1 to 0.5 V) of the peaks makes the polymer a possible candidate as a positive electrode material (i.e., p-doped polymer) in energy storage

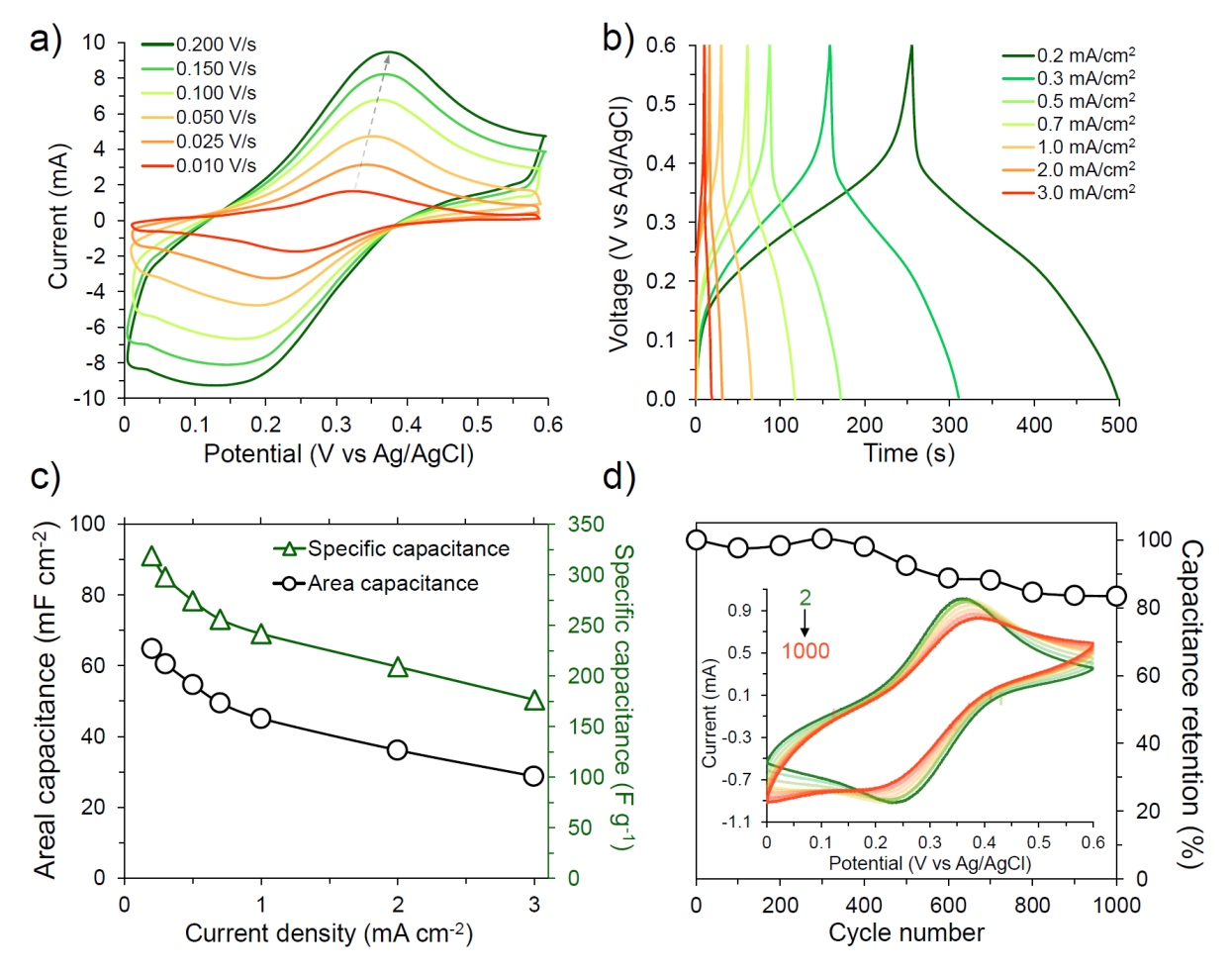
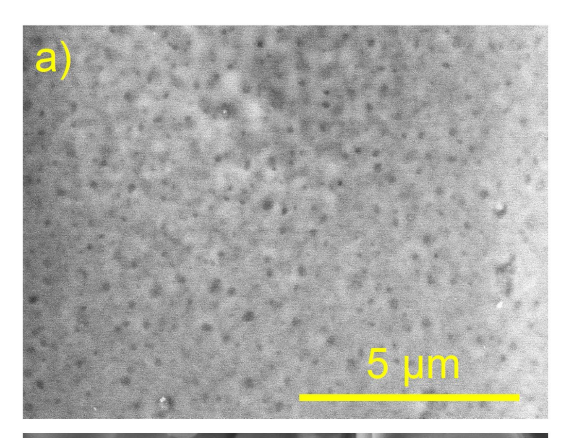


Figure 4. CV curves of the **Cbz-PANI-1**/AU@PET electrode at different scan rates, (a). GCD curves of the **Cbz-PANI-1**/AU@PET electrode at various current densities, (b). Areal capacitances and specific capacitances of **Cbz-PANI-1**/AU@PET at various applied current densities calculated GCD. (c); capacitance retention of the **Cbz-PANI-1**/AU@PET electrode over 1000 CV cycles (inset shows the change in CV after every 100 cycles during extended cycling) (d)

devices. The symmetry between anodic/cathodic peaks indicates good reversibility of the redox reactions during charge/discharge of the polymer electrode. Even when the sweep rate is increased by more than twenty-fold (10 to 200 mV s⁻¹) the position of the oxidative peak shifts only slightly from 0.33 to 0.37 V. Galvanostatic charge discharge (GCD) experiments were performed for the Cbz-PANI-1/Au@PET electrode at various current densities (0.2-5.0 mA cm⁻²) **Figure 4b** and **Figure S6**. Considering the average active material mass loading (i.e., 0.3 mg cm⁻²) the Cbz-PANI-1/Au@PET electrode exhibits a maximum areal capacitance of 64.8 mF cm⁻² and specific capacitance of 319 F g⁻¹ at a current density of 0.2 mA cm⁻² (Figure 4c). The maximum areal capacity and specific capacity were determined to be 13.6 µAh cm⁻² and 53.2 mAh g⁻¹, respectfully (**Figure S7**). In addition, Cbz-PANI-1/Au@PET demonstrates good cyclic stability (i.e., ≈ 83% of capacitance retention) for 1000 CV cycles (Figure 4d inset) between 0.0 and 0.6 V at a scan rate of 200 mV s⁻¹ Figure 4d: thus, indicating that Cbz-PANI-1 has properties suitable for application as a supercapacitor material. Furthermore, the high cycling stability of the polymer coupled with its reversible color change(s) during electrochemical cycling can provide a visual indication of the materials state of charge. These combined properties are highly sought after for developing the next generation of "smart' electrochromic energy storage devices and make **Cbz-PANI** well positioned for such an application.

SEM images of the film before and after 100 CV cycles for **Cbz-PANI-1**/AU@PET electrode was performed to determine any morphology changes of the film. The SEM result of the **Cbz-PANI-1**/AU@PET cycled electrode (**Figure 5**) shows a significant morphological change in the polymer film over the first 100 CV cycles. This morphological change is likely due to the swelling and expanding of the polymer as it undergoes several redox cycles, resulting in change in the overall shape of the CV and GCD curves during/after extended cycling. Likewise, the device shows a slight change in the overall shape of the CV curves after the first 100 cycles (**Figure 6c**) indicating that the morphology change is not completely mitigated by the PVA/H₂SO₄ gel electrolyte.

The fabricated **Cbz-PANI-1**/Au@PET//**Cbz-PANI-1**/Au@PET device exhibits CV curves with the combination of both pseudocapacitive (faradaic) and double-layer (EDLC) type capacitive behaviors over the 0.7 V operating voltage **Figure 6a**. The CV curves of the symmetric device show that most of the charge is being stored between 0.1–0.6 V (in good agreement with the 3-electrode CV results for **Cbz-PANI-1**/Au@PET, **Figure 4a** and **b**). In addition, the current steadily increases as the scan rate increases from 10 to 200 mV s⁻¹ and the overall shape is well maintained: thus, revealing good pseudocapacitive properties of the device. The GCD results give a maximum energy density of 2.45 W



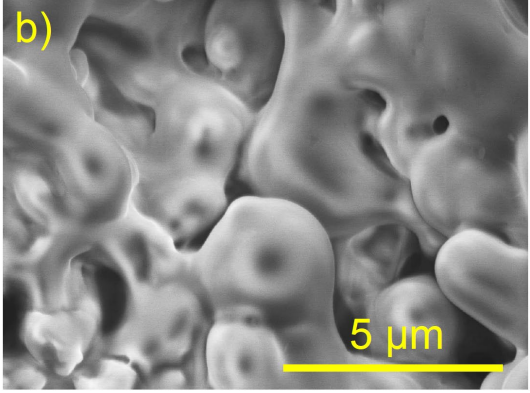


Figure 5. SEM of pristine (a) and cycled spray-coated CBz-PANI-1 electrodes (b).

h kg⁻¹ at 0.2 A g⁻¹, with an energy of 1.06 W h kg⁻¹ being maintained at a high power of 2.71 kW kg⁻¹ (at 10 A g⁻¹). These results demonstrate a good rate capability of the device Figure S8. The device is also able to achieve a high maximum capacitance of 36 F g-1 (9 mF cm-2) and good capacitance retention at higher rates Figure S8c. Unfortunately, extended cycling studies of the initial symmetric **Cbz-PANI-1**/Au@PET/**Cbz-PANI-1**/Au@PET prototype device was rather poor (≈ 45%). Upon further investigation, it was discovered that the poor performance of the device is likely due to poor device handling, i.e., the device showed mechanical instability with over-handling. Therefore, a set of 10 similarly constructed devices were prepared and evaluated for their extended cycling performance. The best device gave excellent cyclability (>91% capacity retention) over 1000 GCD cycles at 0.500 mA cm⁻² (Figure 6c-d). From these results, it is believed that improvement in the long-term cycling performance for Cbz-PANI-1 requires more device optimization. Overall, these results are comparable and even superior to similar symmetric PANI devices made without conductive additives or special structural arrangements, 5, 50 and other CPs from the literature (**Table S4**).⁶⁷⁻⁷⁰ Operationally, when the symmetric device is fully charged the positive electrode becomes fully oxidized while the negative electrode is simultaneously reduced. After discharge, both electrodes reach their half-oxidized states, thereby allowing only 50% of each electrode material's total capacitance to be utilized. Likewise, the operational voltage of the symmetric devices is primarily limited to the potential window of **Cbz-PANI-1**

(\approx 0.6 V). Overall, the symmetric device demonstrates good energy, and power; thus, indicating that **Cbz-PANI-1** is well suited for supercapacitor applications.

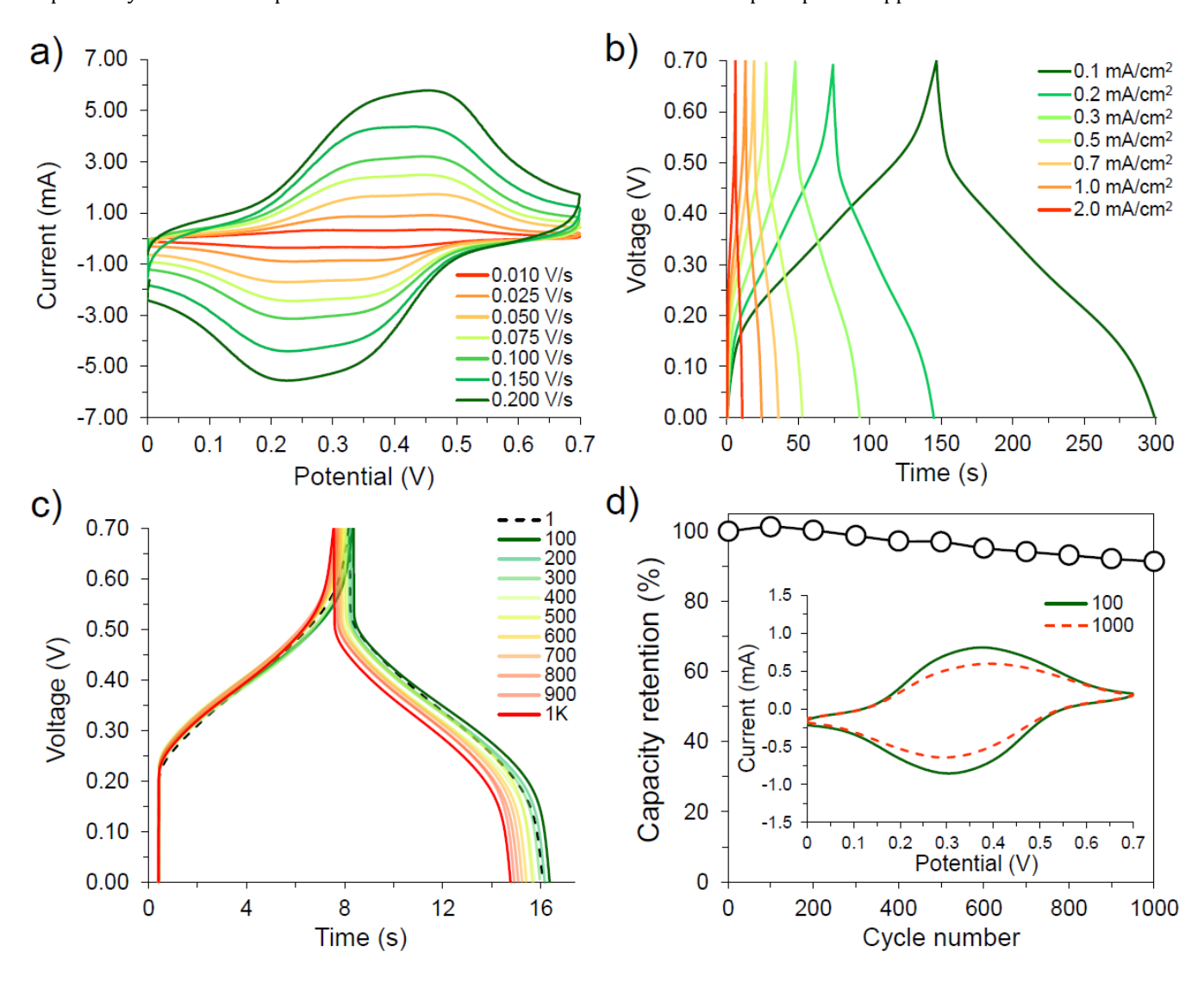


Figure 6. CV curves of the initial symmetric Cbz-PANI-1/Au@PET/Cbz-PANI-1/Au@PET prototype device (individual electrode mass loading = 0.3 mg/cm^2) at various scan rates (a) and its GCD curves at various current densities (b). GCD cycling performance for the best device (mass loading $\approx 0.100 \text{ mg/cm}^2$) (c) and its capacity retention over 1000 GCD cycles at 0.5 mA/cm^2 (Inset shows cyclic voltammogram for the best device after various GCD cycles) (d).

CONCLUSIONS

In summary, two new carbazole-based PANI-derivatives (Cbz-PANI) were successfully synthesized and characterized. The polymers' molecular weights were 18 and 9 kDa for Cbz-PANI-1 and Cbz-PANI-2, respectively. The synthesized polymers mimicked the properties of classical PANI in the UV and EPR spectra of the doped states. The polymers underwent a large bathochromic shift in the absorption spectra when doped similar to PANI. Additionally, they both displayed strong polaronic signals within the EPR spectra. Cbz-PANI-1 (2.8 S cm⁻¹) was found

to be more conductive than **Cbz-PANI-2** (0.70 S cm⁻¹), potentially due to the better film formation of **Cbz-PANI-1**, which has a much higher M_n. Furthermore, **Cbz-PANI-1** displayed electrochromic properties when the electrical potential was increased from 0.0 V to 0.6 V against Ag/AgCl, transitioning from pale yellow/green (analogous PANI eleucoemeraldine form) to green (analogous PANI emeraldine salt), then into blue (analogous PANI pernigraniline salt) when fully oxidized. Unlike classical PANI, **Cbz-PANI-1** was found to be electrochemically stable and processable. **Cbz-PANI-1** was able to achieve a high specific capacitance (319 F g⁻¹) and good electrochemical

stability across a wide potential window of $0-0.6\,\mathrm{V}$ and has been applied as both positive and negative electrode material in an all-polymer symmetric supercapacitor. The side chains and tunable MW of **Cbz-PANI-1** increased the solubility of the polymer, enabling easy processing of **Cbz-PANI-1** via spray coating or drop-casting onto various substrates (i.e., Au@PET and ITO@glass). The **Cbz-PANI-1**//**Cbz-PANI** supercapacitors provide an energy density of $\approx 2.5-1\,\mathrm{W}\,\mathrm{h}\,\mathrm{kg}^{-1}$ and a power density of $0.05-2.7\,\mathrm{kW}\,\mathrm{kg}^{-1}$, which are comparable with similar symmetric SC devices in the literature. Lastly, the electrochromic behavior of this polymer could find application in future "smart" energy storage devices since the state of charge can be visually monitored.

ASSOCIATED CONTENT

Supporting Information. The Supporting Information is available free of charge via the Internet at http://pubs.acs.org." Additional experimental data, calculation and pdf of FTIR, UV, CV, GCD and TGA data are reported.

AUTHOR INFORMATION

Corresponding Author

Colleen N. Scott – Mississippi State University, Department of Chemistry, Mississippi State, Mississippi 39762, United States; orcid.org/0000-0003-3332-2439;

Email: cscott@chemistry.msstate.edu

Authors

Mohammed Almtiri – Mississippi State University, Department of Chemistry, Mississippi State, Mississippi 39762, United States

Timothy J. Dowell – Mississippi State University, Department of Chemistry, Mississippi State, Mississippi 39762, United States; orcid.org/0000-0002-0339-4258 Hari Giri – Mississippi State University, Department of Chemistry, Mississippi State, Mississippi 39762, United States

David O. Wipf – Mississippi State University, Department of Chemistry, Mississippi State, Mississippi 39762, United States; orcid.org/0000-0003-2365-1175

Author Contributions

MA and TJD contributed equally.

Funding Sources

The authors are grateful for the financial support from the National Science Foundation for award (CHE-1945503).

Notes

The authors declare no competing financial interest base on the findings of this work.

REFERENCES

- 1. Mustafin, A. G.; Latypova, L. R.; Andriianova, A. N.; Mullagaliev, I. N.; Salikhov, S. M.; Salikhov, R. B.; Usmanova, G. S., Polymerization of new aniline derivatives: synthesis, characterization and application as sensors. *RSC Advances* **2021**, *11* (34), 21006-21016.
- 2. Kazemi, F.; Naghib, S. M.; Zare, Y.; Rhee, K. Y., Biosensing Applications of Polyaniline (PANI)-Based Nanocomposites: A Review. *Polym. Rev.* **2021,** *61* (3), 553-597.
- 3. Flouda, P.; Quinn, A. H.; Patel, A. G.; Loufakis, D.; Lagoudas, D. C.; Lutkenhaus, J. L., Branched aramid nanofiber-polyaniline electrodes for structural energy storage. *Nanoscale* **2020**, *12* (32), 16840-16850.
- 4. Eftekhari, A.; Li, L.; Yang, Y., Polyaniline supercapacitors. *J. Power Sources* **2017**, *347*, 86-107.
- 5. Huang, Z.; Ji, Z.; Feng, Y.; Wang, P.; Huang, Y., Flexible and stretchable polyaniline supercapacitor with a high rate capability. *Polym Int* **2021**, *70* (4), 437-442.
- 6. Kong, P.; Feng, H.; Chen, N.; Lu, Y.; Li, S.; Wang, P., Polyaniline/chitosan as a corrosion inhibitor for mild steel in acidic medium. *RSC Advances* **2019**, *9* (16), 9211-9217.
- 7. Zhang, Y.; Shao, Y.; Liu, X.; Shi, C.; Wang, Y.; Meng, G.; Zeng, X.; Yang, Y., A study on corrosion protection of different polyaniline coatings for mild steel. *Prog. Org. Coat.* **2017**, *111*, 240-247.
- 8. Rangel-Olivares, F. R.; Arce-Estrada, E. M.; Cabrera-Sierra, R., Synthesis and Characterization of Polyaniline-Based Polymer Nanocomposites as Anti-Corrosion Coatings. *Coatings* **2021**, *11* (6), 653.
- 9. Zeng, M.; Zhu, W.; Luo, J.; Song, N.; Li, Y.; Chen, Z.; Zhang, Y.; Wang, Z.; Liang, W.; Guo, B.; Zhang, K.; Huang, F.; Cao, Y., Highly Efficient Nonfullerene Organic Solar Cells with a Self-Doped Water-Soluble Neutral Polyaniline as Hole Transport Layer. *Solar RRL* **2021**, *5* (3), 2000625.
- 10. Al-Dainy, G. A.; Watanabe, F.; Kannarpady, G. K.; Ghosh, A.; Berry, B.; Biris, A. S.; Bourdo, S. E., Optimizing Lignosulfonic Acid-Grafted Polyaniline as a Hole-Transport Layer for Inverted CH(3)NH(3)PbI(3) Perovskite Solar Cells. *ACS Omega* **2020**, *5* (4), 1887-1901.
- 11. Kwiatkowska, E.; Mech, W.; Wincukiewicz, A.; Korona, K. P.; Zarębska, K.; Kamińska, M.; Skompska, M., Investigation of polyaniline doped with camphorsulfonic acid in chloroform solution as a hole transporting layer in PTB7: PCBM and perovskite-based solar cells. *Electrochimica Acta* **2021**, *380*, 138264.
- 12. Gupta, T. K.; Singh, B. P.; Mathur, R. B.; Dhakate, S. R., Multi-walled carbon nanotube–graphene–polyaniline multiphase nanocomposite with superior electromagnetic shielding effectiveness. *Nanoscale* **2014**, *6* (2), 842-851.
- 13. Zou, L.; Lan, C.; Yang, L.; Xu, Z.; Chu, C.; Liu, Y.; Qiu, Y., The optimization of nanocomposite coating with polyaniline coated carbon nanotubes on fabrics for exceptional electromagnetic interference shielding. *Diam. Relat. Mater.* **2020**, *104*, 107757.
- 14. Marmisollé, W. A.; Inés Florit, M.; Posadas, D., Electrochemically induced ageing of polyaniline. An electrochemical impedance spectroscopy study. *J. Electroanal. Chem.* **2012**, *673*, 65-71.
- 15. Arsov, L. D.; Plieth, W.; Koßmehl, G., Electrochemical and Raman spectroscopic study of polyaniline; influence of the potential on the degradation of polyaniline. *J Solid State Electrochem*; **1998**, *2* (5), 355-361.

- 16. Mažeikien≐, R.; Malinauskas, A., Electrochemical stability of polyaniline. *Eur. Polym. J* **2002**, *38* (10), 1947-1952
- 17. Geng, Y.; Jing, X.; Wang, F., Solution properties of doped polyaniline. *J. Macromol. Sci. Phys. Part B* **1997**, *36* (1), 125-135.
- 18. Cao, Y.; Smith, P.; Heeger, A. J., Counter-ion induced processibility of conducting polyaniline and of conducting polyblends of polyaniline in bulk polymers. *Synth. Met.* **1992**, *48* (1), 91-97.
- 19. Jeon, J.-W.; Ma, Y.; Mike, J. F.; Shao, L.; Balbuena, P. B.; Lutkenhaus, J. L., Oxidatively stable polyaniline:polyacid electrodes for electrochemical energy storage. *Phys. Chem. Chem. Phys.* **2013**, *15* (24), 9654-9662.
- 20. Mooss, V. A.; Vijayakumar, V.; Kurungot, S.; Athawale, A. A., Interconnected polyaniline nanostructures: Enhanced interface for better supercapacitance retention. *Polymer.* **2021**, *212*, 123169.
- 21. Almtiri, M.; Dowell, T. J.; Chu, I.; Wipf, D. O.; Scott, C. N., Phenoxazine-Containing Polyaniline Derivatives with Improved Electrochemical Stability and Processability. *ACS Appl. Polym. Mater.* **2021**, *3* (6), 2988-2997.
- 22. Dumur, F., Carbazole-based polymers as hosts for solution-processed organic light-emitting diodes: Simplicity, efficacy. *Org. Electron.* **2015**, *25*, 345-361.
- 23. Boudreault, P.-L. T.; Beaupré, S.; Leclerc, M., Polycarbazoles for plastic electronics. *Polym. Chem.* **2010**, *1* (2), 127-136.
- 24. Grazulevicius, J. V.; Strohriegl, P.; Pielichowski, J.; Pielichowski, K., Carbazole-containing polymers: synthesis, properties and applications. *Prog. Polym. Sci.* **2003**, *28* (9), 1297-1353.
- 25. Siove, A.; Adès, D., Synthesis by oxidative polymerization with FeCl3 of a fully aromatic twisted poly(3,6-carbazole) with a blue-violet luminescence. *Polymer* **2004**, *45* (12), 4045-4049.
- 26. Kumar, A.; Tiwari, M.; Prakash, R., Electrochemical Study of Interfacially Synthesized Polycarbazole with Different Oxidants. *ChemElectroChem* **2015**, *2* (12), 2001-2010.
- 27. Morin, J.-F.; Leclerc, M., Syntheses of Conjugated Polymers Derived from N-Alkyl-2,7-carbazoles. *Macromolecules* **2001**, *34* (14), 4680-4682.
- 28. Hu, B.; Li, C.; Liu, Z.; Zhang, X.; Luo, W.; Jin, L., Synthesis and multi-electrochromic properties of asymmetric structure polymers based on carbazole-EDOT and 2, 5–dithienylpyrrole derivatives. *Electrochim. Acta* **2019**, *305*, 1-10.
- 29. Sung, M. J.; Kim, K.; Kwon, S.-K.; Kim, Y.-H.; Chung, D. S., Phenanthro[110,9,8-cdefg]carbazole-Thiophene, Donor–Donor Copolymer for Narrow Band Green-Selective Organic Photodiode. *J. Phys. Chem C* **2017**, *121* (29), 15931-15936.
- 30. Mansha, M.; Mehmood, U.; Ullah, N., Poly(phenylene cyanovinylenes) carbazole based conjugated polymer as a photosensitizer for dye-sensitized solar cells. *Mater. Lett.* **2018**, *231*, 56-59.
- 31. Bhuvana, K. P.; Bensingh, R. J.; Kader, M. A.; Nayak, S. K., Polymer Light Emitting Diodes: Materials, Technology and Device. *Polym Plast Technol Eng* **2018**, *57* (17), 1784-1800.
- 32. Karon, K.; Lapkowski, M., Carbazole electrochemistry: a short review. *J. Solid State Electrochem.* **2015**, *19* (9), 2601-2610.
- 33. Saraswathi, R.; Gerard, M.; Malhotra, B. D., Characteristics of aqueous polycarbazole batteries. *J. Appl. Polym. Sci.* **1999**, *74* (1), 145-150.
- 34. Qian, J.; Zhang, Y.; Liu, X.; Xia, J., Carbazole and fluorene polyaniline derivatives: Synthesis, properties and application

- as multiple stimuli-responsive fluorescent chemosensor. *Talanta* **2019**, *204*, 592-601.
- 35. Simon, P.; Gogotsi, Y., Materials for electrochemical capacitors. *Nat Mater* **2008**, *7* (11), 845-54.
- 36. Poonam; Sharma, K.; Arora, A.; Tripathi, S. K., Review of supercapacitors: Materials and devices. *J. Energy Storage* **2019**, *21*, 801-825.
- 37. Sohan, A.; Banoth, P.; Aleksandrova, M.; Nirmala Grace, A.; Kollu, P., Review on MXene synthesis, properties, and recent research exploring electrode architecture for supercapacitor applications. *Int. J. Energy Res.* **2021**, *45* (14), 19746-19771.
- 38. Khani, H.; Wipf, D. O., Iron Oxide Nanosheets and Pulse-Electrodeposited Ni–Co–S Nanoflake Arrays for High-Performance Charge Storage. *ACS Appl. Mater. Interfaces* **2017**, *9* (8), 6967-6978.
- 39. Šedajová, V.; Jakubec, P.; Bakandritsos, A.; Ranc, V.; Otyepka, M., New Limits for Stability of Supercapacitor Electrode Material Based on Graphene Derivative. *Nanomaterials* **2020**, *10* (9), 1731.
- 40. Fong, K. D.; Wang, T.; Smoukov, S. K., Multidimensional performance optimization of conducting polymer-based supercapacitor electrodes. *Sustain. Energy Fuels* **2017**, *1* (9), 1857-1874.
- 41. Shown, I.; Ganguly, A.; Chen, L.-C.; Chen, K.-H., Conducting polymer-based flexible supercapacitor. *Energy Sci. Eng.* **2015**, *3* (1), 2-26.
- 42. Snook, G. A.; Kao, P.; Best, A. S., Conducting-polymer-based supercapacitor devices and electrodes. *J. Power Sources* **2011**, *196* (1), 1-12.
- 43. Khani, H.; Dowell, T. J.; Wipf, D. O., Modifying Current Collectors to Produce High Volumetric Energy Density and Power Density Storage Devices. *ACS Appl. Mater. Interfaces* **2018**, *10* (25), 21262-21280.
- 44. Liu, L.; Tian, F.; Zhou, M.; Guo, H.; Wang, X., Aqueous rechargeable lithium battery based on polyaniline and LiMn2O4 with good cycling performance. *Electrochimica Acta* **2012**, *70*, 360-364.
- 45. Soni, R.; Kashyap, V.; Nagaraju, D.; Kurungot, S., Realizing High Capacitance and Rate Capability in Polyaniline by Enhancing the Electrochemical Surface Area through Induction of Superhydrophilicity. *ACS Appl. Mater. Interfaces* **2018**, *10* (1), 676-686.
- 46. Wang, X.; Wu, D.; Song, X.; Du, W.; Zhao, X.; Zhang, D., Review on Carbon/Polyaniline Hybrids: Design and Synthesis for Supercapacitor. *Molecules* **2019**, *24* (12), 2263..
- 47. Hong, X.; Fu, J.; Liu, Y.; Li, S.; Wang, X.; Dong, W.; Yang, S., Recent Progress on Graphene/Polyaniline Composites for High-performance Supercapacitors. *Materials* **2019**, *12* (9), 1451
- 48. Wang, Y.-G.; Li, H.-Q.; Xia, Y.-Y., Ordered Whiskerlike Polyaniline Grown on the Surface of Mesoporous Carbon and Its Electrochemical Capacitance Performance. *Adv. Mater.* **2006**, *18* (19), 2619-2623.
- 49. Yang, Y.; Chen, C.; Li, D., Electrodes based on cellulose nanofibers/carbon nanotubes networks, polyaniline nanowires and carbon cloth for supercapacitors. *Mater. Res. Express* **2018**, *6* (3), 035008.
- 50. Xie, Y.; Liu, Y.; Zhao, Y.; Tsang, Y. H.; Lau, S. P.; Huang, H.; Chai, Y., Stretchable all-solid-state supercapacitor with wavy shaped polyaniline/graphene electrode. *J. Mater. Chem. A* **2014**, *2* (24), 9142-9149.
- 51. Pan, C.; Gu, H.; Dong, L., Synthesis and electrochemical performance of polyaniline @MnO2/graphene ternary composites for electrochemical supercapacitors. *J. Power Sources* **2016**, *303*, 175-181.

- 52. Guan, R.; Xu, Y.; Ying, L.; Yang, W.; Wu, H.; Chen, Q.; Cao, Y., Novel green-light-emitting hyperbranched polymers with iridium complex as core and 3,6-carbazole-co-2,6-pyridine unit as branch. *J. Mater. Chem.* **2009**, *19* (4), 531-537.
- 53. Iraqi, A.; Waturu, I., Preparation of poly(9-alkylcarbazole-3,6-diyl)s via palladium catalysed cross-coupling reactions. *Synth. Met.* **2001**, *119* (1), 159-160.
- 54. Wolfe, J. P.; Buchwald, S. L., Scope and Limitations of the Pd/BINAP-Catalyzed Amination of Aryl Bromides. *J. Org. Chem.* **2000**, *65* (4), 1144-1157.
- 55. Wolfe, J. P.; Wagaw, S.; Marcoux, J.-F.; Buchwald, S. L., Rational Development of Practical Catalysts for Aromatic Carbon–Nitrogen Bond Formation. *Acc. Chem. Res.* **1998**, *31* (12), 805-818.
- 56. Tian, J.; Wang, G.; Qi, Z.-H.; Ma, J., Ligand Effects of BrettPhos and RuPhos on Rate-Limiting Steps in Buchwald–Hartwig Amination Reaction Due to the Modulation of Steric Hindrance and Electronic Structure. *ACS Omega* **2020**, *5* (34), 21385-21391.
- 57. Moon, D. K.; Ezuka, M.; Maruyama, T.; Osakada, K.; Yamamoto, T., Kinetic study on chemical oxidation of leucoemeraldine base polyaniline to emeraldine base. *Macromolecules* **1993**, *26* (2), 364-369.
- 58. Kang, Y.-T.; Wang, C.-C.; Chen, C.-Y., Preparation of 2D leaf-shaped and 3D flower-shaped sandwich-like polyaniline nanocomposites and application on anticorrosion. *J. Appl. Polym. Sci.* **2021**, *138* (4), 49729.
- 59. Moraes, I. R.; Kalbáč, M.; Dmitrieva, E.; Dunsch, L., Charging of Self-Doped Poly(Anilineboronic Acid) Films Studied by in Situ ESR/UV/Vis/NIR Spectroelectrochemistry and ex Situ FTIR Spectroscopy. *ChemPhysChem* **2011**, *12* (16), 2920-2924.
- 60. Patil, S.; Chougule, M.; Pawar, S.; Sen, S.; Patil, D. V., Effect of Camphor Sulfonic Acid Doping on Structural, Morphological, Optical and Electrical Transport Properties on Polyaniline-ZnO Nanocomposites. *Soft Nanosci. Lett.* **2012**, *2*. 61. Stejskal, J.; Kratochvíl, P.; Radhakrishnan, N., Polyaniline dispersions 2. UV—Vis absorption spectra. *Synth. Met.* **1993**,

61 (3), 225-231.

- 62. Gupta, S. K.; Luthra, V.; Singh, R., Electrical transport and EPR investigations: A comparative study for d.c. conduction mechanism in monovalent and multivalent ions doped polyaniline. *Bull. Mater. Sci.* **2012**, *35* (5), 787-794.
- 63. Krinichnyi, V. I.; Roth, H. K.; Schrödner, M.; Wessling, B., EPR study of polyaniline highly doped by p-toluenesulfonic acid. *Polymer* **2006**, *47* (21), 7460-7468.
- 64. Choi, J.; Kim, W.; Kim, D.; Kim, S.; Chae, J.; Choi, S. Q.; Kim, F. S.; Kim, T.-S.; Kim, B. J., Importance of Critical Molecular Weight of Semicrystalline n-Type Polymers for Mechanically Robust, Efficient Electroactive Thin Films. *Chem. Mater.* **2019**, *31* (9), 3163-3173.
- 65. Albuquerque, J. E.; Mattoso, L.; Balogh, D. T.; Faria, R.; Masters, J.; MacDiarmid, A., A simple method to estimate the oxidation state of polyanilines. *Synth. Met.* **2000**, *113*, 19-22. 66. de Albuquerque, J. E.; Mattoso, L. H. C.; Faria, R. M.;
- Masters, J. G.; MacDiarmid, A. G., Study of the interconversion of polyaniline oxidation states by optical absorption spectroscopy. *Synth. Met.***2004**, *146* (1), 1-10.
- 67. Österholm, A. M.; Ponder, J. F.; Kerszulis, J. A.; Reynolds, J. R., Solution Processed PEDOT Analogues in Electrochemical Supercapacitors. *ACS Appl. Mater. Interfaces* **2016**, *8* (21), 13492-13498.
- 68. Guo, Y.; Li, W.; Yu, H.; Perepichka, D. F.; Meng, H., Flexible Asymmetric Supercapacitors via Spray Coating of a New Electrochromic Donor–Acceptor Polymer. *Adv. Energy Mater.* **2017**, *7* (2), 1601623.
- 69. Sun, Y.; Zhu, G.; Zhao, X.; Kang, W.; Li, M.; Zhang, X.; Yang, H.; Guo, L.; Lin, B., Solution-processable, hypercrosslinked polymer via post-crosslinking for electrochromic supercapacitor with outstanding electrochemical stability. *Sol. Energy Mater. Sol. Cells* **2020**, *215*, 110661.
- 70. Wang, K.; Huang, L.; Eedugurala, N.; Zhang, S.; Sabuj, M. A.; Rai, N.; Gu, X.; Azoulay, J. D.; Ng, T. N., Wide Potential Window Supercapacitors Using Open-Shell Donor–Acceptor Conjugated Polymers with Stable N-Doped States. *Adv. Energy Mater.* **2019**, *9* (47), 1902806.

For Table of Contents Only

